Resonant electronic Raman scattering in optimally doped $Bi_2Sr_2CaCu_2O_{8+x}$ superconductor

2000 J. Phys.: Condens. Matter 12 9095

(http://iopscience.iop.org/0953-8984/12/42/314)

J. Phys.: Condens. Matter **12** (2000) 9095–9105. Printed in the UK PII: S0953-8984(00)13637-9

Resonant electronic Raman scattering in optimally doped $Bi_2Sr_2CaCu_2O_{8+x}$ superconductor

O V Misochko† and E Ya Sherman‡

† Institute of Solid State Physics, Russian Academy of Sciences, 142432 Chernogolovka, Moscow Region, Russia

‡ Moscow Institute of Physics and Technology, 141700 Dolgoprudny, Russia

Received 2 May 2000

Abstract. We report experimental results on resonant electronic Raman scattering in superconducting single crystals of $Bi_2Sr_2CaCu_2O_{8+x}$. The change of excitation wavelength results in a shift of the position for the superconductivity-induced 2Δ peak in A_{1g} and B_{1g} symmetries. In addition, in the red-light excitation a new Raman peak arises at approximately 130 K in the B_{1g} spectra. Various explanations of these effects are discussed.

1. Introduction

Raman scattering in high-T_c superconductors has turned out to be a powerful technique for studying the properties of phonons and electronic excitations. A common feature of the experimental data obtained by means of Raman scattering in high-T_c superconductors is a broad and strong electronic continuum that redistributes itself below T_c into relatively sharp, symmetry-dependent peaks [1]. The overall shape of the electronic Raman spectrum and its temperature and doping dependence are not fully understood. Nevertheless, a large body of investigation ascribes the peaks in the electronic Raman scattering as a manifestation of the momentum-dependent superconducting gap $\Delta(\boldsymbol{k}) = \Delta f(\boldsymbol{n}_F)$, where $\boldsymbol{n}_F$ is the direction of the Fermi momentum, and uses the peak position to measure the magnitude of the superconducting order parameter Δ [1, 2]. However, direct identification of the peak position with 2Δ is clouded even for the B_{1g} scattering symmetry, because of the unknown origin of the electronic continua [3]. Recall that Raman spectroscopy is an optical technique, and the results of measurements depend on photon frequency. Indeed, resonance effects for the position of the 2Δ peak have been observed in several high-T_c compounds [4, 5].

It is reasonable to assume that there are some spectral features which can be seen in the Raman experiments for one photon energy while they are hidden for another one. Such features could be ascribed to excitations related to certain parts of the Brillouin zone and the Fermi surface. If the incident photon energy is close to interband transition points in these parts of the Brillouin zone, the probability of excitation will be strongly enhanced. Therefore, resonant Raman experiments are indispensable for the investigation of the excitations localized in momentum space.

To clarify what kind of such excitations could be observed in resonant Raman scattering, let us recall that in the last decade numerous attempts were made to explain the high-T_c superconductivity within the Bose–Einstein condensation (BEC) scenario [6–9]. This scenario finds some support in several experiments, carried out primarily on underdoped samples,

0953-8984/00/429095+11$30.00

which evidence the formation of a pseudogap at $T^* > T_c$ [10, 11]. The apparent discrepancy between the wide fluctuation range inherent to BEC and the sharp Bardeen–Cooper–Schrieffer (BCS) transition is removed when BEC occurs against a Fermi liquid background [9]. In this case the preformed pairs are formed by the states close to the Van Hove singularity—that is, localized in the momentum space. This effect makes the BEC suitable for investigation by resonant Raman spectroscopy. If the combined BEC–BCS scenario contains essential physics, it should be traceable to optimally doped samples. In this case, by changing the doping level, one can follow a crossover from BEC at low carrier concentration to a BCS scenario at higher doping. For the underdoped regime, Raman data for B_{1g} symmetry have revealed a peak persisting into the normal state. The peak was attributed to the formation of a bound state associated with precursor pairing above T_c [10, 11]. However, later this viewpoint was challenged by the observation of an oxygen-isotope-induced shift for the crystals away from optimum doping [12]. Compelling evidence for BEC at high carrier concentration is still lacking.

Here we report a resonance Raman study on a nearly optimally doped Bi2212 superconductor for different temperatures and light polarizations. The observed behaviour of the 2Δ peaks suggests that the superconducting state cannot be fully described by a BCS-like theory with a $d_{x^2-y^2}$ gap where the electron pairing causes an instability of the *entire* Fermi surface at T_c with no anomaly present at a higher temperature.

2. Experimental results

Details of the Bi2212 crystal characterization and a description of the experimental set-up are given elsewhere [13]. What is important for this study is that the crystal was single phase and homogeneous, as checked by x-ray and Raman microprobes. The magnetically measured $T_c = 89$ K showed that the crystal was close to optimum doping. A relatively narrow transition width ($\sim$3 K) confirmed its high quality.

The Raman spectra were taken at two excitation wavelengths: violet ($\lambda_v = 458$ nm, $\hbar\omega_v = 2.72$ eV) and red ($\lambda_r = 633$ nm, $\hbar\omega_r = 1.95$ eV) provided by either an Ar or a He–Ne laser. The spectra were measured in a quasi-backscattering geometry from the crystal glued with silver paste on the cold finger of an optical helium cryostat. The scattered light dispersed with a resolution better than 4 cm^{-1} provided by a triple Raman spectrometer was detected by a nitrogen-cooled charge-coupled-device detector. All spectra were corrected for the detector-plus-optical-system response and normalized for laser intensity. To avoid overheating of the crystal, the laser power density at the sample was low (of the order of 10 W cm^{-2}). Moreover, the laser intensity was kept constant within the whole temperature run for each polarization. The temperatures referred to in the paper are the nominal temperatures inside the cryostat. However, even with the low laser intensity we cannot exclude the possibility of a minor overheating of order 10 K in the superconducting state, detection of which was beyond our accuracy, limited by a Stoke/anti-Stokes method. The laser beam was made incident on the crystal surface at the Brewster angle, to minimize elastically scattered light. The position of the laser spot, whose diameter did not exceed 150 μm, was controlled with an accuracy of about 10–20 μm by means of a microscope attachment. The coordinate system used to specify the symmetry components is chosen to be locked to the CuO bonds of the CuO_2 plane, and irreducible representations are of the tetragonal point group. The imaginary part of the response function, $\chi''(\Omega, T)$, was obtained by Bose factorization of the experimental spectral density of the scattered light, $\rho(\Omega, T)$, for the two are related via the fluctuation-dissipation theorem: $\rho(\Omega, T) \sim [1 - \exp(-\hbar\Omega/T)]^{-1}\chi''(\Omega, T)$.

The $x'y'$-spectrum, coupled to the excitations of B_{1g} symmetry, undergoes a significant alteration in the superconducting state for both laser wavelengths; see figure 1(a). However, what is interesting is that the continuum, observed at the lowest attainable temperature, peaks at different frequencies when the spectra are excited by the violet and the red laser lines. The shift in frequency for the 2Δ peaks can also be inferred from the interception points, shown by dashed lines, where the superconducting- and normal-state spectra merge.

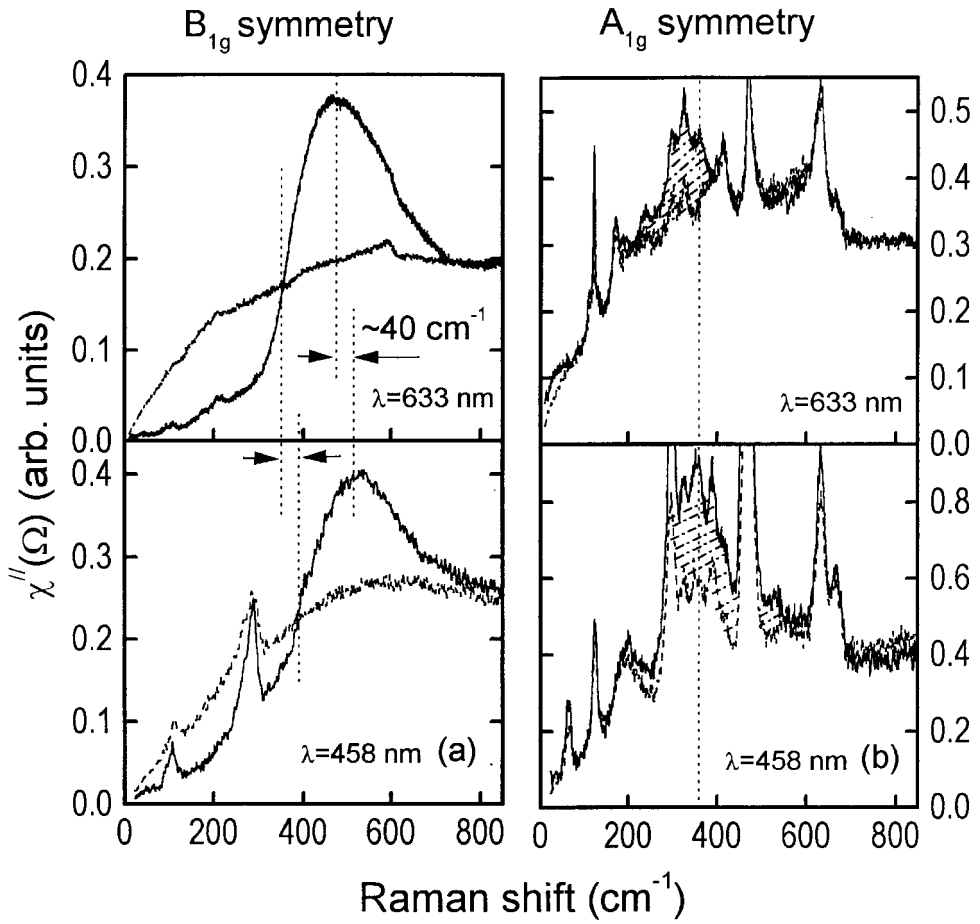

Figure 1. B_{1g} (a) and A_{1g} (b) response functions of Bi2212 above ($T = 90$ K, dashed lines) and below ($T = 10$ K, solid lines) $T_c = 89$ K measured at $\lambda = 633$ and $\lambda = 458$ nm. The dashed lines in the left panel mark the maxima and interception points for the B_{1g} symmetry. The hatched areas in the right panel represent the 2Δ peaks for the A_{1g} symmetry, while the dashed line marks the maximum for the violet, $\lambda = 458$ nm, excitation.

A similar shift in the peak position with λ most probably exists also for the A_{1g} symmetry, which was derived from the xx- and $x'y'$-spectra and is shown in figure 1(b). Although the A_{1g} spectrum is spoiled by the phonons superimposed on the electronic continuum, the behaviour of the centres of gravity of the 2Δ peaks, which can serve as a measure of the peak positions, suggests that the peaks are located at different frequencies for the two laser wavelengths. Note that the positions of the strong A_{1g} phonon peaks remain unchanged for the two excitation wavelengths. The 2Δ peak shift for different photon energies can be inferred from the data

of Kang *et al* [4] on Tl2201 compounds and Sacuto *et al* [5] on Hg1223 compounds. Note that our results and those of Sacuto *et al* [5] demonstrate a similar trend: the peak frequency increases with the decrease of λ.

Since the phonons and electronic continuum resonate in the B_{1g} channel differently, the B_{1g} spectrum at $\lambda = 633$ nm consists of a pure electronic contribution. This phonon-free spectrum makes it possible to observe a peak in the electronic continuum above T_c. Absent at room temperature, a peak appears between 200 and 150 K and can be clearly seen at $T = 130$ and 90 K, as presented in figure 2. This peak, centred at 595 cm^{-1}, is strongly asymmetric, being much steeper on the high-frequency side. When the temperature is further decreased, the 595 cm^{-1} peak gains in intensity, to almost merge at the lowest temperature with the peak that occurs at T_c at a lower ($\sim$465 cm^{-1}) frequency. It has to be added that although we could not trace the detailed temperature evolution of the 2Δ peak at A_{1g} symmetry because of the phonons, our data show that the integrated spectral weight included in the sum rule for Raman scattering:

$$\chi''_{\rm int}(T) \sim \int \Omega \left[\chi''(\Omega, T) - \chi''(\Omega, T_c)\right] \, {\rm d}\Omega \tag{1}$$

for the two, A_{1g} and B_{1g}, symmetries substantially increases for $T \leqslant T_c$.

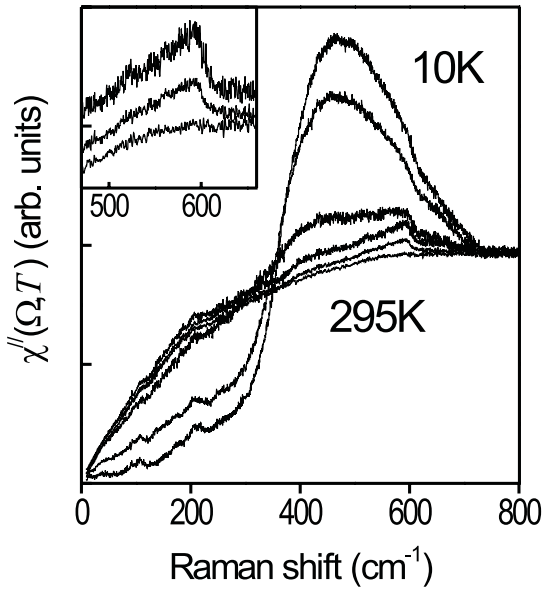

Figure 2. The temperature evolution of the B_{1g} response function taken with $\lambda = 633$ nm. The temperature $T = 10, 40, 80, 90, 130, 295$ K from top to bottom. The inset shows a magnified view of the spectra at $T = 295, 130$, and 90 K.

From a close inspection of figure 2, we infer that the 2Δ peak positions are almost temperature independent in the superconducting state. Lending strength to the temperature independence is the fact that the interception points, which can be measured with a high accuracy, vary by less than 10% from $T = 90$ K down to $T = 10$ K. To illustrate the gap evolution, we plot in figure 3 the normalized peak position as a function of temperature. As is evident from figure 3, the gap measured from the maximum of the peak develops more sharply than would be expected from a weak-coupling BCS theory. At the same time, the scattering intensity in the pile-up shows approximately linear behaviour, $\chi''_{\rm int}(T) \sim T - T_c$,

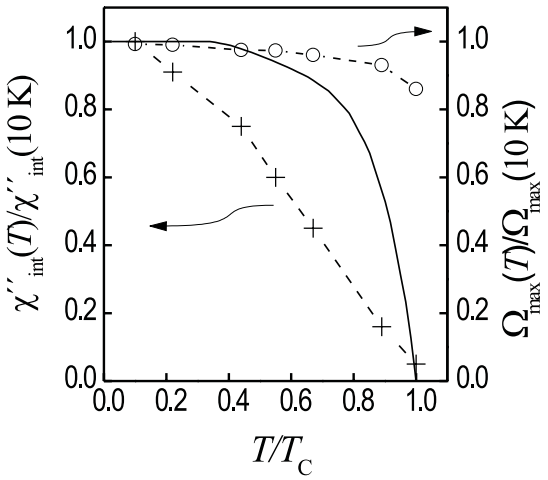

Figure 3. The temperature dependence of the normalized 2Δ peak frequency and of the normalized integrated intensity in the B_{1g} channel. The solid line is the weak-coupling BCS temperature dependence for the superconducting gap.

for temperatures $T > T_c/3$—that is, the scattering follows the number of paired particles in the superconducting state [14]. Study of a few Bi2212 crystals at doping close to the optimum ($T_c = 89$–91 K) has confirmed the general trend clearly seen in figure 3. Our result that the temperature dependence of the gap deviates substantially from the BCS form is in agreement with the data obtained for Y123, Bi2212, La214, and Tl2201 [15–18].

3. Discussion

There are two interesting aspects of our results that require explanation. The first is the double-peak structure of the 2Δ peak and the appearance of a high-frequency component of the structure above T_c. The second aspect is the shift of the 2Δ peak, observed for different laser wavelengths. Both of these features are related to resonant properties of Raman scattering.

Let us start with the double-mode structure of the 2Δ peak, observed for the red laser excitation. The low-frequency component appearing at T_c and gaining in intensity in the *superconducting* state is ascribed to pair-breaking excitations. The high-frequency component, absent at room temperature while present well above T_c, opens up two different possibilities for its assignment. The high-frequency peak can be ascribed to the phonon, or, alternatively, associated with the excitation of the electronic subsystem.

Let us first discuss the phonon origin of the peak. The high frequency of the peak hints at an oxygen stretching mode being responsible for it. There are two A_{1g} stretching vibrations in the crystal under study, arising from the z-axis displacement of the oxygen ions surrounding the Bi ion [19]. These are clearly seen in the A_{1g} spectra and have different frequencies and lineshapes. There are also E_g stretching vibrations [20], but the off-diagonal phonons are usually very weak even in the allowed (xz- or yz-) polarizations for high-T_c superconductors [21], and for Bi2212 have been not detected so far. The last possibility is an infrared-active mode made Raman active by disorder. However, for the disordered crystal, the 'regular' (not disorder-induced) fully symmetric phonons can 'leak' into forbidden B_{1g} polarization. The corresponding ratio of intensities for two-dimensional carriers can be estimated as $I(B_{1g})/I(A_{1g}) \sim \ln(k_F\ell)/k_F\ell$, where ℓ is the electron free path, and k_F is the Fermi momentum [22]. Within our experimental

accuracy, no regular A_{1g} phonon leaks to the forbidden polarization. This observation testifies against strong disorder. As a consequence, the probability for the observation of disorder-induced phonons is low. Additionally, we note that one is more likely to observe phonons in the violet light than in the red one due to a resonance effect, and the disorder-induced phonons, since they do not obey specific selection rules, should be observed in polarized spectra, too.

Recently it was reported that in the samples strongly underdoped by oxygen removal with $T_c \approx 51$ K, the 590 cm^{-1} feature demonstrates a partial oxygen isotope shift thus supporting its defect-induced phonon origin [12]. On the basis of the partial isotope shift and the absence of the feature in Y-substituted samples with approximately the same doping level, the 590 cm^{-1} peak was assigned to the *b*-axis stretching vibrations of oxygen atoms in the Bi–O layer. There are, however, some difficulties in the identification of the 590 cm^{-1} peak in the underdoped crystals with our 595 cm^{-1} peak seen at the optimal doping. To name a few: the lineshape of the 590 cm^{-1} peak observed by Hewitt *et al* is either symmetric or exhibits a small asymmetry, being steeper on the *low-frequency* side, whereas our peak is very asymmetric with a much steeper *high-frequency* slope. The 590 cm^{-1} peak is already present at room temperature and the temperature decrease only mildly affects its peak intensity relative to the electronic background or other phonons (see figure 1 in reference [12]). This has to be contrasted with the absence of our peak at room temperature and the strong temperature dependence that starts well above T_c, continuing into the superconducting state. Moreover, the Raman spectrum of optimally doped crystal, presented by Hewitt *et al* [12] (see figure 3 in reference [12]), perfectly matches our data in terms of both phonon and electronic peak frequencies. Thus, at optimal doping there is no disorder-induced phonon at the given frequency.

The last possibility for assigning the feature to a phonon is to consider the possibility of multiphase inclusions in our crystals—that is, the crystal being essentially optimally doped but with some regions at lower doping levels. Again, there are a number of points militating against such a multiphase situation. First, nowhere in the crystals do we observe phonon frequencies characteristic of the strongly underdoped phase. Second, the electronic spectrum at B_{1g} symmetry in the underdoped state is strongly suppressed in intensity. Therefore, we can exclude the situation where we probe different phases at different temperatures, since the strength of the electronic continua at high frequency shifts is constant in our data within the experimental accuracy. We recall here that the position of the laser spot was controlled in our experiment with accuracy better than 10% of the spot size. Therefore, we can discard the possibility of inhomogeneous composition in lateral dimensions. However, we have to consider the possibility that our crystal could have some inhomogeneity perpendicular to the crystal surface—that is, the oxygen content and disorder varying along the *c*-axis. If we assume that the light penetration depth is significantly smaller for the red laser light than for the violet one, we can explain the appearance of the disorder-induced phonon under red excitation since the depleted oxygen layer makes the major contribution for the latter. Note that in this case the shift in frequency for the 2Δ peak could be explained by the different doping level. Nevertheless, even with such inhomogeneity the whole set of our data can be explained only if the penetration depth is significantly smaller for the light polarized at 45° relative the CuO bonds than along the bonds. Indeed, the frequencies of fully symmetric phonons perfectly match those for optimally doped crystal at any laser excitation, which testifies that at least for this polarization we probe the same phase with both excitation wavelengths.

On the basis of the given analysis, we suppose that for the optimally doped, high-quality crystals the peak at 595 cm^{-1} can have some electronic rather than phononic origin. A similar peak in the normal state has been reported by Quilty *et al* when the spectra for underdoped, optimally doped, and overdoped Bi2212 were taken in the same symmetry channel but with a green laser line [23]. However, these authors did not observe the double-mode

structure of the peak in the superconducting state, probably because of the different resonance conditions and of the fact that only the ratio of the superconducting to the normal spectra was analysed.

Now let us consider possible electronic candidates for producing the peak. A double-mode structure of the Raman spectra at B_{1g} symmetry arising due to the Van Hove singularity in the electronic spectrum of the CuO_2 planes was predicted by Branch and Carbotte [24] for the *superconducting* state. These authors [24] used the effective-mass approximation for the Raman vertex to point out that, in addition to the pair-breaking peak, the second spectral feature could arise due to the singularity. The spectral position of this feature strongly depends on band-structure parameters. Yet, for the optimally doped crystals, the approach of Branch and Carbotte [24] predicts a single-mode behaviour, since the singularity falls at the Fermi surface for optimal doping. The double-mode structure for the B_{1g} channel at $\lambda = 633$ nm can be interpreted within the bound-state scenario suggested by Blumberg *et al* [10]. Note however that this scenario was advocated primarily for the underdoped regime and our data seem to contradict the suggestion that cooling below T_c merely increases the occupation of the bound state, resulting in a coherence over the whole Fermi surface. The cooling has a much more pronounced effect on the lower-frequency peak of the double-mode structure, which gains in intensity more sharply in the superconducting state.

To understand the situation, let us start with the resonant two-band Raman vertex, which in the B_{1g} polarization has the form

$$\begin{aligned}\gamma_{B_{1g}}(\boldsymbol{k},\omega) &\equiv \gamma'_{B_{1g}}(\boldsymbol{k},\omega) + i\gamma''_{B_{1g}}(\boldsymbol{k},\omega)\\ &\propto \left(|\langle f,\boldsymbol{k}|\hat{p}_x|i,\boldsymbol{k}\rangle|^2 - |\langle f,\boldsymbol{k}|\hat{p}_y|i,\boldsymbol{k}\rangle|^2\right)\\ &\quad\times\left[\frac{1}{E_F - E_i(\boldsymbol{k}) - \omega - i\Gamma} + \frac{1}{E_F - E_i(\boldsymbol{k}) + \omega - i\Gamma}\right]. \qquad (2)\end{aligned}$$

Here $\hat{\boldsymbol{p}}$ is the momentum operator, $E_i(\boldsymbol{k})$ is the initial band energy, where $\boldsymbol{k}$ is the electron momentum near the Fermi surface, and Γ is the lifetime broadening. We have set $\hbar = 1$ and assumed that the Fermi level E_F intersects the band denoted as f. At the Brillouin zone diagonal—that is, at $\boldsymbol{k}_d = (\pm k_F/\sqrt{2}, \pm k_F/\sqrt{2})$ points—$\gamma_{B_{1g}}(\boldsymbol{k}_d,\omega) = 0$. Thus, the $\boldsymbol{k}$-dependence of the vertex is important in the vicinity of the diagonals. The resonance effect can either enhance or weaken the $\boldsymbol{k}$-dependence of $\gamma_{B_{1g}}(\boldsymbol{k},\omega)$. Indeed, as we can see in equation (2), if $|E_F - E_i(\boldsymbol{k}) - \omega|$ decreases (increases) along the Fermi surface near the $\boldsymbol{k}_d$-points, the $\boldsymbol{k}$-dependence becomes more (less) pronounced. Furthermore, the $\boldsymbol{k}$-dependence over the entire Fermi surface can be modified when E_F approaches the extended Van Hove singularity observed in Bi2212 [27]. Above T_c, the electronic Raman continuum at zero momentum transfer is only due to elastic and/or inelastic relaxation of the excitations characterized by a time $\tau_{\boldsymbol{k}}$ [28,29]. Near a resonance, the photon with frequency ω probes relaxation rates mainly in a part of the Fermi surface where $E_F - E_i(\boldsymbol{k})$ is close to ω. In some sense, a change in photon frequency is analogous to the change of scattering polarization. As is known, the B_{1g} channel probes mainly the states near the BZ axes, the B_{2g} the states near the BZ diagonals, whereas the A_{1g} probes the states over the entire Fermi surface (albeit in a screened way) [1]. However, under altered resonance conditions, the states with wavevectors $\boldsymbol{k}$ within the region chosen by a given scattering channel can be differently weighted. As first pointed out for Y123, Raman scattering in the B_{1g} channel measures the regions with high relaxation rate, whereas in the A_{1g} symmetry those with a substantially smaller relaxation rate are probed [30]. Such a ratio of the relaxation rates, observed also for the B_{1g} and B_{2g} channels in Bi2212 [31], suggests strongly anisotropic quasiparticle scattering.

In the normal state, the Raman susceptibility at low frequencies is a linear function of the Raman shift: $\chi''(\Omega) \sim \Omega\zeta_L(\omega)$ with L specifying the symmetry channel. The value of $\zeta_L(\omega)$

can roughly be estimated as $N_F\langle\tau_{\boldsymbol{k}}\gamma_L^2(\boldsymbol{k},\omega)\rangle$, where $\langle\cdots\rangle$ denotes averaging over the Fermi surface, and N_F is the density of states at E_F [28]. Since the slope of $\chi''(\Omega\to 0, T)$ weakly depends on temperature in the normal state, we argue that the scattering of the quasiparticles is mainly elastic, without either the magnetic pseudoscaling observed in a slightly overdoped La124 crystal [32] or a pseudogap. Thus, antiferromagnetic fluctuations do not contribute substantially to the relaxation rate and Raman scattering in our crystal. We note that within the 'scattering-rate' approach, the appearance of the new peak at $\Omega\sim 600\ \mathrm{cm}^{-1}$ would imply that the contribution of the Fermi surface states, characterized by an inverse relaxation time $\tau_{\boldsymbol{k}}^{-1}\sim 600\ \mathrm{cm}^{-1}$, to the total density of states is substantially increased. However, such an increase at $T\approx 100$ K seems to be unlikely. Moreover, this redistribution of states would lead to a change of the static Raman slope at the same temperature, which is not detected within the experimental uncertainty. Therefore, we conclude that a new scattering channel not related to momentum relaxation is opened up at $T\geqslant T_c$ in *a part* of the Fermi surface.

To understand the resonance-induced shift of the peak position, let us consider Raman scattering in the normal and superconducting state in more detail. In the pioneering work by Abrikosov and Fal'kovskii [33] the comparison of Raman efficiencies for the normal and superconducting states revealed that the efficiency is a universal function of $\Omega/2\Delta$ with the maximum position scaling as Δ^{-1} at $T=0$. As a next step, Klein and Dierker pointed out that even within the BCS scenario the situation could be quite complicated and considerably dependent on the ratio between the light penetration depth and coherence length [34]. No analysis of resonance Raman scattering was given in either of the two basic papers. For $T\ll\Delta$, we have in the zero-momentum-transfer limit the Raman susceptibility in a clean superconductor

$$\chi''_{\mathrm{B_{1g}}}(\Omega, T\to 0)=\frac{N_F}{\Omega}\,\mathrm{Re}\left\langle\frac{\left|\gamma_{\mathrm{B_{1g}}}(\omega,\boldsymbol{k})\right|^2|\Delta(\boldsymbol{k})|^2}{\sqrt{\Omega^2-4|\Delta(\boldsymbol{k})|^2}}\right\rangle. \tag{3}$$

As our experiments show, the low-frequency portion of the spectra is appreciably distinct for different photon energies. For higher Ω, the portion of the Fermi surface where $\Omega>2|\Delta(\boldsymbol{k})|$ is increased. As a result, $\chi''_{\mathrm{B_{1g}}}(\Omega, T\to 0)$ is substantially determined by the $\boldsymbol{k}$-dependence of both $\gamma_{\mathrm{B_{1g}}}(\omega,\boldsymbol{k})$ and $\Delta(\boldsymbol{k})$. The static slope $\partial\chi''_{\mathrm{B_{1g}}}(\Omega,T)/\partial\Omega$ at $\Omega\to 0$ is larger for $\lambda=458$ nm, with the peak intensities being approximately equal for $\lambda=458$ and 633 nm; see figure 1. At the same time, the 2Δ peak is a bit sharper at larger λ, being shifted by $\approx$40 cm^{-1} downward with respect to the violet excitation. From these experimental observations, we can draw two conclusions. The first is that the narrowing of the 2Δ peak suggests that $\gamma_{\mathrm{B_{1g}}}(\omega,\boldsymbol{k})$ for the larger λ increases rapidly towards the $(0,k_F)$ point—that is, to the maximal gap states. In a superconductor without relaxation of quasiparticles, equation (3) yields a very sharp maximum in $\chi_{\mathrm{B_{1g}}}(\Omega,T)$ at $\Omega=2\Delta$ for any $\gamma_{\mathrm{B_{1g}}}(\omega,\boldsymbol{k})$ due to a sharp increase in the density of states at this energy. Therefore, ω-dependence of the 2Δ peak arises due to relaxation of the excitations. If both $\gamma_{\mathrm{B_{1g}}}(\omega,\boldsymbol{k})$ and $|\Delta(\boldsymbol{k})|$ were monotonic, reaching maxima at the BZ axes, the Raman intensity would have peaked at 2Δ independently of the photon energy. Thus, our second conclusion is that either $\gamma_{\mathrm{B_{1g}}}(\omega,\boldsymbol{k})$ or $\Delta(\boldsymbol{k})$ or both of them are non-monotonic in the $0<\theta<\pi/4$ range, where θ is the angle between $\boldsymbol{k}$ and the BZ axis. The dependence of $\gamma_{\mathrm{B_{1g}}}(\omega,\boldsymbol{k})$ is controlled by the band-structure parameters and photon frequency. To illustrate this dependence, we consider the Raman vertex within a three-band tight-binding model analogous to that of reference [35]. Figure 4 gives an example of the ω-dependence of the imaginary and real parts of the Raman vertex. The red light is in resonance with interband transitions near the Van Hove singularity, and, therefore, probes the excitations in this part of the Brillouin zone. Also, the gap $\Delta(\boldsymbol{k})$—even when it is of $\mathrm{d}_{x^2-y^2}$ symmetry—can reach a maximum of $|\Delta(\boldsymbol{k})|$ not on the high-symmetry directions, $(0,\pm k_F)$

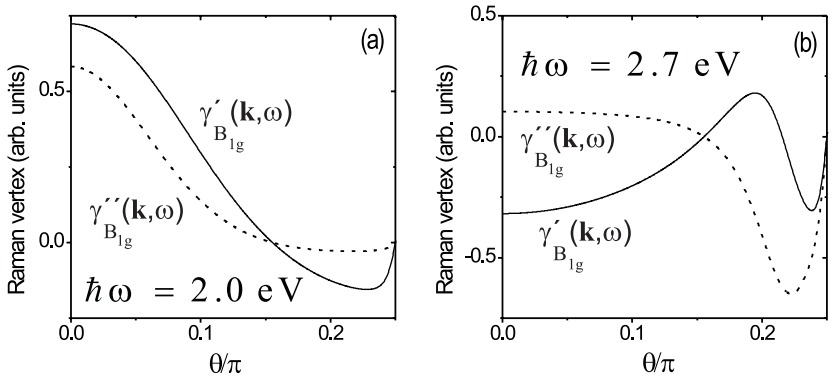

Figure 4. The Raman vertex $\gamma_{B_{1g}}$ for red (a) and violet (b) light. Dashed and solid lines represent the imaginary and real parts, respectively. The tight-binding model parameters are chosen as: $\varepsilon_{pd} = 0$, $t_{pd} = 0.8$ eV, $t_{pp} = 0.7$ eV (ε_{pd} is the difference between the Cu and O site energies; t_{pd} and t_{pp} are the Cu–O and O–O hopping, respectively). The Fermi level intersects the upper band made by the antibonding combination of Cu and O orbitals. The concentration of electrons $\langle n\rangle = 0.85$ corresponds to the optimum doping. The lifetime broadening $\Gamma = 0.15$ eV. The figure merely illustrates the possibility of a strongly ω-dependent non-monotonic Raman vertex even for a simple band-structure model.

and $(\pm k_F, 0)$, but slightly off these lines. The latter may be somewhat analogous to a gap with nodes shifted from the BZ diagonals [5]. At the present time we cannot decide between these two possibilities.

4. Conclusions

Provided that the double-mode structure and the shift of the 2Δ peak are not the trivial effect of disordered and multiphase crystals, the following tentative scenario seems to be consistent with our experimental observations. The electron pairs form above T_c due to a binding of fermions to bosons near the extended Van Hove singularity. Such a binding is possible [9] when BEC occurs against the background of a Fermi liquid. Near the extended Van Hove singularity, the large anisotropy of the effective mass leads to the pairing above T_c even at rather weak coupling. The pairing is not necessarily related to antiferromagnetic fluctuations since no magnetic pseudoscaling is observed in our experiment. The relaxation processes only weakly mix the bosons with the states away from singularity since the quasiparticle scattering amplitude is strong only for small scattering angles. With the $\lambda = 633$ nm photons, which are supposed to be in resonance with the interband transition near the $(0, k_F)$-like points, a normal-state pair-breaking peak at the frequency close to the boson binding energy can be seen. The preformed pairs occupy only a small portion of the Fermi surface near the singularity. This smallness is responsible for the fact that the low-frequency part of the Raman spectra remains unchanged when the peak is formed. We should mention that the peak energy is not related directly to the position of the singularity; however, to have the singularity in the electronic structure it is necessary for Cooper pair preformation to be possible.

The temperature dependence of the boson-induced peak is controlled by two competing effects. First, the occupation number and size of the 'bosonized' region should grow at lower temperatures, as pointed out in reference [10]. This results in a moderate increase of the 595 cm^{-1} peak intensity, observed below T_c. However, the bound states can be destroyed by a participation in the ordinary (BCS) pairing of fermions in the superconducting state. Within

our scenario, the superconducting gap formed below T_c should be strongly anisotropic because the pairing, effective mass, and relaxation rate of fermions are all strongly $\boldsymbol{k}$-dependent. Being a feature developed over the entire Fermi surface, the superconducting gap is clearly seen at any frequency of the exciting light. The superconducting gap is large on the Fermi surface parts where the B_{1g} Raman vertex is large, so in a Raman experiment for this symmetry it appears as if the gap grows very rapidly at $T < T_c$.

To sum up the results, we have investigated the resonant properties of the electronic Raman scattering in Bi2212 superconductor. For the red excitation we have observed that the 2Δ peak at B_{1g} symmetry exhibits a composite structure with one of its components appearing above T_c. We have also observed that at different resonance conditions the superconductivity-induced peaks are centred at different frequencies for both A_{1g} and B_{1g} symmetries and confirmed the peculiar temperature dependence of both the frequency and the intensity of the 2Δ peak. Two possible explanations for the observed anomalies have been considered. The first is a trivial multiphase structure of the crystals with some disordered regions at slightly smaller doping. The second possibility is preformed electronic pairs capable of explaining the double-mode structure and, additionally, dependent on the photon energy weighting in $\boldsymbol{k}$-space accounting for the resonance-induced shift. With the data at hand, we are compelled to consider the second explanation more plausible.

We should mention an interesting similarity between our data and infrared (IR) light absorption spectroscopy. The IR results of van der Marel *et al* [36] show that the superconducting gap in $YBa_2Cu_3O_7$ opens much faster than is predicted by BCS theory. Another similarity observed recently in $HgBa_2Ca_2Cu_3O_{8+\delta}$ by McGuire *et al* [37] is related to a scaling between the superconducting gap and T_c.

Acknowledgment

We are grateful to C Kendziora for valuable discussions. EYS is indebted to C Ambrosch-Draxl, N Bontemps, R Combescot, P Monod and A Sacuto for interesting converstions and to the Austrian Science Fund for support of the project M534-TPH.

References

[1] Devereaux T P, Einzel D, Stadlober B, Hackl R, Leach D H and Neumeier J J 1994 *Phys. Rev. Lett.* **72** 396
[2] Strohm T and Cardona M 1997 *Phys. Rev.* B **55** 12 725
[3] Chen X K, Altendorf E, Irwin J C, Liang R and Hardy W N 1993 *Phys. Rev.* B **48** 10 530
Kendziora C, Kelley R J and Onellion M 1996 *Phys. Rev. Lett.* **77** 727
[4] Kang M, Blumberg G, Klein M V and Kolesnikov N N 1996 *Phys. Rev. Lett.* **77** 4434
[5] Sacuto A, Combescot R, Bontemps N, Müller C A, Viallet V and Colson D 1998 *Phys. Rev.* B **58** 11 721
[6] Alexandrov A S 1993 *Phys. Rev.* B **48** 10 571
[7] Emery V and Kivelson S 1995 *Phys. Rev. Lett.* **74** 3253
[8] Ioffe L B and Millis A J 1996 *Phys. Rev.* B **54** 3645
[9] Geshkenbein V, Ioffe L and Larkin A I 1997 *Phys. Rev.* B **55** 3173
[10] Blumberg G, Kang M, Klein M V, Kadowaki K and Kendziora C 1997 *Science* **278** 1427
[11] Nemetschek R R, Opel M, Hoffmann C, Muller P F, Hackl R, Berger H, Forro L, Erb A and Walker E 1997 *Phys. Rev. Lett.* **78** 4837
Puchkov A V, Fournier P, Basov D N, Timusk T, Kapitulnik A and Kolesnikov N N 1996 *Phys. Rev. Lett.* **77** 3212
King D M, Shen Z-X and Dessau D S 1996 *J. Phys. Chem. Solids* **56** 1865
Takigawa M 1991 *Phys. Rev.* B **42** 243
[12] Hewitt K C, Wang N L, Irwin J C, Pooke D M, Pantoja A E and Trodahl H J 1999 *Phys. Rev.* B **60** R9943
[13] Misochko O V and Genda G 1997 *Physica* C **228** 115
Misochko O V 1998 *Fiz. Tverd. Tela* **40** 998 (Engl. Transl. 1998 *Russ. Phys.–Solid State* **40** 914)

[14] Misochko O V 1999 *Solid State Commun.* **113** 141
[15] Hackl R, Gläser W, Müller P, Einzel D and Andres K 1988 *Phys. Rev.* B **38** 7133
[16] Yamanaka A, Takato H, Minami F, Inoue K and Takekawa S 1992 *Phys. Rev.* B **46** 516
Staufer T, Nemetschek R, Hackl R, Muller P and Veith H 1992 *Phys. Rev. Lett.* **68** 1069
[17] Chen X K, Irwin J C, Trodahl H J, Okuya M, Kimura T and Kishio K 1998 *Physica* C **295** 80
[18] Gasparov L V, Lemmens P, Brinkman M, Kolesnikov N N and Güntherodt G 1997 *Phys. Rev.* B **52** 13 652
[19] Liu R R, Klein M V, Han P D and Payne D A 1992 *Phys. Rev.* B **45** 7392
Pantoja A E, Pooke D M, Trodahl H J and Irwin J C 1998 *Phys. Rev.* B **58** 5219
[20] Prade J, Kulkarni A D, de Wette F W, Schröder U and Kress W 1989 *Phys. Rev.* B **39** 2771
[21] Gasparov L V, Kulakovskii V D, Misochko O V and Timofeev V B 1989 *Physica* C **157** 341
McCarty K F, Liu J Z, Shelton R N and Radousky H B 1990 *Phys. Rev.* B **41** 8792
[22] Misochko O V and Sherman E Ya 1994 *Physica* C **222** 219
[23] Quilty J W, Trodahl H J and Pooke D M 1998 *Phys. Rev.* B **57** R11 097
[24] Branch D and Carbotte J P 1995 *Phys. Rev.* B **52** 603
Branch D and Carbotte J P 1996 *Phys. Rev.* B **54** 13 288
[25] Misochko O V and Sherman E Ya 1998 *Int. J. Mod. Phys.* B **12** 2455
[26] Ma J, Quitmann C, Kelley R J, Almäras P, Berger H, Margaritondo G and Onellion M 1995 *Phys. Rev.* B **51** 3832
[27] Sherman E Ya 1998 *Phys. Rev.* B **58** 14 187
[28] Zawadowski A and Cardona M 1990 *Phys. Rev.* B **42** 10 732
[29] Jiang C and Carbotte J P 1996 *Phys. Rev.* B **53** 11 868
[30] Slakey F, Klein M V, Rice J P and Ginsberg D M 1991 *Phys. Rev.* B **43** 3764
[31] Hackl R, Opel M, Müller P F, Krug G, Stadlober B, Nemetschek R, Berger H and Forro L 1996 *J. Low Temp. Phys.* **105** 733
[32] Naeini J G, Chen X K, Hewitt K C, Irwin J C, Devereaux T P, Okuya M, Kimura T and Kishio K 1998 *Phys. Rev.* B **57** R11 077
[33] Abrikosov A A and Fal'kovskii L A 1961 *Zh. Eksp. Teor. Fiz.* **40** 262 (Engl. Transl. 1961 *Sov. Phys.–JETP* **13** 179)
[34] Klein M V and Dierker S B 1984 *Phys. Rev.* B **29** 49 769
[35] Opel M, Hackl R, Devereaux T P, Virosztek A, Zawadowski A, Erb A, Walker E, Berger H and Forro L 1999 *Phys. Rev.* B **60** 9836
[36] van der Marel D *et al* 1991 *Phys. Rev.* B **43** 8606
van der Marel D *et al* 1991 *Physica* C **180** 112
[37] McGuire *et al* 1999 *Preprint* cond-mat/9912338